

Frequency-Domain Fluorescence Lifetime Measurements via Frequency Segmentation and Recombination as Applied to Pyrene with Dissolved Humic Materials

Hadi M. Marwani · Mark Lowry · Baoshan Xing ·
Isiah M. Warner · Robert L. Cook

Received: 22 December 2007 / Accepted: 21 April 2008 / Published online: 11 June 2008
© Springer Science + Business Media, LLC 2008

Abstract In this study, the association behavior of pyrene with different dissolved humic materials (DHM) was investigated utilizing the recently developed segmented frequency-domain fluorescence lifetime method. The humic materials involved in this study consisted of three commercially available International Humic Substances Society standards (Suwannee River fulvic acid reference, SRFAR, Leonardite humic acid standard, LHAS, and Florida peat humic acid standard, FPHAS), the peat derived Amherst humic acid (AHA), and a chemically bleached Amherst humic acid (BAHA). It was found that the three commercial humic materials displayed three lifetime components, while both Amherst samples displayed only two lifetime components. In addition, it was found that the chemical bleaching procedure preferentially removed red wavelength emitting fluorophores from AHA. In regards to pyrene association with the DHM, different behavior was

found for all commercially available humics, while AHA and BAHA, which displayed strikingly similar behavior in terms of fluorescence lifetimes. It was also found that there was an enhancement of pyrene's measured lifetime (combined with a decrease in pyrene emission) in the presence of FPHAS. The implications of this long lifetime are discussed in terms of (1) quenching mechanism and (2) use of the fluorescence quenching method used to determine the binding of compounds to DHM.

Keywords Time-resolved fluorescence · Environment · Hydrophobic organic compound · Static · Dynamic · Stern–Volmer · Curvature · Data analysis

Introduction

Humic materials (HM) are omnipresent within the environment [1, 2] and play a range of functions, including impacting the fate and transport of hydrophobic organic compounds (HOC). This has led to a great amount of interest in how HOC interact with HM. Various models have been proposed, but no one model has been universally accepted, as exemplified by the vigorous discussion of the “glassy/rubber” (hard/soft or condensed/non-condensed) model in the literature [3–8]. Even the once almost universally agreed upon concept that HOC sorb into aromatic domains within HM [9–15], has recently been questioned [16–18]. Thus, the seemingly simple questions in regards to how HM associate with HOC are still open.

At the root of this apparent confusion is the complex, heterogeneous, polydisperse and molecular assembly nature of HM [1, 19]. Due to the nature of HM, the association of HOC with DHM should be studied (1) by as non-intrusive analytical method as possible, (2) at as close to “in-situ”

Electronic supplementary material The online version of this article (doi:10.1007/s10895-008-0377-3) contains supplementary material, which is available to authorized users.

H. M. Marwani · M. Lowry · I. M. Warner · R. L. Cook (✉)
Department of Chemistry, Louisiana State University,
Baton Rouge, LA 70803, USA
e-mail: rlcook@lsu.edu

H. M. Marwani
Department of Chemistry, King Abdulaziz University,
Jeddah 21589, Saudi Arabia

B. Xing
Department of Plant, Soil and Insect Sciences, Stockbridge Hall,
University of Massachusetts,
Amherst, MA 01003, USA

R. L. Cook
Department of Chemistry, Southern University at Baton Rouge,
Baton Rouge, LA 70813, USA

conditions as possible, and (3) at as close to environmentally relevant concentrations as possible. Many fluorescence methods, some prominent in bioanalytical chemistry [20], are also highly amenable to studying dissolved humic materials (DHM). Gauthier et al. [21] introduced the use of fluorescence probe quenching (FQ) to determine equilibrium constants for the association of fluorescent HOC with DHM via Stern–Volmer plots. Though extremely common, the FQ method is not without limitations and controversy. The major bone of contention is that this technique assumes a complete static quenching of the fluorescence probe when it associates with the DHM. A large body of evidence is beginning to emerge which questions this assumption, such as: (1) the positive curvature in Stern–Volmer plots [22–26]; (2) the observation that the FQ method yields higher association constants than other methods [23–25, 27]; (3) the use of pyrene to study the polarity of humic substances [28, 29], and (4) evidence for a partial quenching of fluorescence probes by HM [30]. These four points are consistent with a combination of static and dynamic quenching, rather than the assumed dark static quenching mechanism. Other limitations of the FQ technique include: (A) the assumption that the probe's fluorescence is linearly dependent on DHM concentrations [26], (B) a possibility of an unaccounted for quenching due to the presence of oxygen [31], and (C) photobleaching of the observed probe's fluorescence [21, 24, 31]. In one such example, Tiller and Jones [31] have indicated that oxygen and long exposure to radiation can overestimate association constants of HOC with DHM. To a certain level, these limitations can be overcome by: (i) keeping the concentration of the DHM constant [26]; (ii) thoroughly degassing the solution under study with an inert gas such nitrogen or argon, and (iii) controlling the fluence level of the excitation source.

The question as to whether the quenching mechanism of HOC by DHM is static, dynamic, or a combination, can be investigated by: (a) exploring the abovementioned upward curvature with Stern–Volmer plots; (b) studying temperature dependence of fluorescence (however, due to the assembly nature of HM, the validity of this method is questionable); and (c) fluorescence lifetime measurements. While the fluorescence lifetime measurements constitute the method of choice, they are sometimes prone to photobleaching, thus complicating data analysis and interpretation for complex systems such as mixtures of HOC with DHM [32]. This factor may explain the conflicting fluorescence lifetime results that support either a very minor [33, 34] or a significant [15, 35] influence of dynamic quenching in the fluorescence quenching of HOC by DHM. Thus, whether the quenching mechanism of HOC with DHM is static, dynamic, or both is still an open question.

In the present study, frequency-domain fluorescence lifetime measurements via frequency segmentation and

recombination were applied to examine the chemical effect of DHM on the association behavior with pyrene—a common fluorescence probe and model HOC. This newly developed technique has been shown to address photobleaching effects [32], as shutter control is not an option for minimizing them in lifetime-based measurement. In addition, experimental considerations—such as the effect of oxygen and wall adsorption—were addressed in order to carefully quantify recovered lifetimes and fractional intensity contributions (i.e. the portion of fluorescence signal from the mixture resulting from either pyrene or humic).

Experimental section

Materials Suwannee River fulvic acid reference (SRFAR), Leonardite humic acid standard (LHAS), and Florida peat humic acid standard (FPHAS), were purchased from the International Humic Substances Society (IHSS), Department of Soil, Water, and Climate, University of Minnesota (St. Paul, MN). The Amherst humic acid (AHA) and a chemically bleached Amherst humic acid (BAHA) following the method of Gunasekara et al. [36] where peat derived. Pyrene ($\geq 99\%$) was obtained from Sigma-Aldrich (Milwaukee, WI, USA) and used as received.

Sample preparation Standard reference solutions of 12, 16, 20, and 24 ppm DHM as well as a standard reference solution of 0.1 ppm pyrene (below its water solubility limit) were prepared in 18.2 M Ω -cm distilled deionized water. Pyrene and DHM mixtures containing 0.04 ppm pyrene and 12, 16, 20, and 24 ppm DHM were prepared at the same experimental conditions of the standard reference solutions and stored in the dark at 4 °C. Mixtures were allowed to equilibrate in the dark for at least seven days. The pH of the solution was adjusted to 5 to create hydrophobic domains within the DHM to associate with pyrene, using dilute NaOH and HCl solutions. All solutions were also allowed to equilibrate overnight in a quartz fluorometer cell equipped with a septum cap, and rinsed with fresh solutions prior to fluorescence measurements. Pyrene, DHM and their mixture solutions were purged using argon gas for exactly 15 min, followed by 5 min equilibration time in the sample compartment with a flow of argon gas over the course of fluorescence measurements. Fluorescence lifetime measurements were also collected for air-equilibrated samples of 24 ppm LHAS to evaluate the effect of oxygen on the recovered fractional intensity contributions and lifetimes of DHM.

Methods The concentration of DHM was verified by total carbon (TC) content analysis using a Shimadzu model TOC-5050A analyzer with an ASI-5000A autosampler

(Kyoto, Japan). Fluorescence measurements were acquired using a Spex Fluorolog-3 spectrofluorometer (model FL3–22TAU3; HORIBA Jobin Yvon, Edison, NJ, USA) equipped with a 450-W xenon lamp and R928P photomultiplier tube (PMT) detector. Fluorescence measurements were made at room temperature in a 10 mm quartz fluorescence cell equipped with a septum cap. The excitation wavelengths were 333 nm for pyrene, DHM, and their mixtures. For characterization of AHA and BAHA, three-dimensional excitation–emission matrices (EEM) fluorescence spectra were collected. The bandwidths for both excitation and emission were 4 nm with integration time of 0.2 s. The excitation (Ex) wavelength was varied from 250 to 550 nm in 5 nm intervals, while the emission (Em) spectra were collected to 600 nm in 1 nm intervals. In addition, absorption spectra were collected and used for correction of both primary and secondary inner-filter effects [20]. Absorbance measurements were performed using the UV-3101PC (UV-VIS-NIR) scanning spectrophotometer (Shimadzu, Columbia, MD, USA).

Frequency-domain fluorescence signals were passed through a 370 nm long-pass filter. Fluorescence lifetime measurements of pyrene and DHM individual components were performed as single long runs, in which the frequency range was 0.5 up to 275.4 MHz, the number of frequencies was 39, and the integration time was 15 s. The frequency segmentation and recombination method consisted of four individual segments, with a fresh solution used for each segment, and was applied to pyrene with DHM mixtures. The number of frequencies for segments 1, 2, 3, and 4 is 13 (4.3–233.3 MHz), 12 (0.5–19.3 MHz), 6 (0.6–3.1 MHz), and 8 (26.9–275.4 MHz), respectively. The integration times were 15 s for segments 1 and 2, 30 s for segment 3, and 7.5 s for segment 4. The data from four segments were recombined onto a single frequency-domain data set for analysis. The number of averages for both long and combined runs was 5, and was calculated using the interleave function, such that an average was generated each time the automated sample turret rotated. The experimental details of both long and combined runs, and the criteria for their selection, were fully described elsewhere by Marwani et al. [32]. Frequency-domain lifetime measurements were collected for all solutions versus ludox—a scatter reference solution—with a lifetime of zero. Frequency-domain phase and modulation decay profiles were analyzed using the Globals software package developed at the Laboratory for Fluorescence Dynamics at the University of Illinois at Urbana-Champaign [37, 38]. Several initial guesses for Nonlinear Least Squares (NLLS) parameters were implemented to evaluate the stability of χ^2 minimization and avoid local minima in the χ^2 surface. Phase and modulation data sets were well fit by appropriate models, and the quality of the fit was judged by visual

inspection of residual plots as well as by χ^2 statistics. Recovered lifetime parameters (lifetimes and fractional intensity contributions) were not strongly dependent upon the choice of errors in the data analyses. Therefore, as is commonly practiced, constant errors of 0.5° and 0.005 were used in analyses for consistency and ease of day-to-day data interpretation [20].

A valid model should usually provide a χ^2 value between 1 and 2 if the constant errors used in the analyses match exactly the degree of error found in the experimental data. However, in the case of difficult/dim samples it may not be possible to obtain χ^2 values within this range. In such cases, spurious χ^2 values alone cannot be used to statistically reject a model and residuals must be taken into consideration in model discrimination. Data fitting details are provided in Marwani et al. [32] and in the “[Results and discussion](#)” section below.

Results and discussion

Lifetime measurements of DHM

Though not fully understood, the exact sorption mechanism between HOC and DHM is likely to involve weak associations—such as hydrophobic interactions—between HOC and DHM. Because of the complex molecular assembly nature of DHM it is important to first gain a better understanding of the DHM itself. Therefore, both recovered fractional contributions and lifetimes of DHM were first evaluated using fluorescence lifetime measurements (Figs. 1 and 2). In this study, the effect of DHM concentration on the recovered fractional contributions and lifetimes was also investigated for argon degassed aqueous solutions of all DHM at different concentrations with the exception of BAHA. The BAHA was obtained by chemically bleaching the AHA using hypochlorous acid (HOCl), resulting in the removal of a large percentage of rigid aromatic moieties and retaining the aliphatic species [36]. Therefore, BAHA is less fluorescent as compared to other DHM (~20% of unbleached AHA), and its fluorescence lifetime measurements were performed at the highest concentration.

A three component model has consistently emerged as the best model for a wide range of DHM and concentrations [39–42]. Consequently, the DHM within our study were expected to each yield three lifetime components. The results for our NLLS analyses were obtained by allowing both the fractional intensity contributions and lifetimes to vary but linking (L) the lifetimes at different concentrations for each humic acid. In this study, the triple-exponential decay (DDD) model was found to be consistent with multi-exponential lifetimes of the commercial (SRFAR, LHAS,

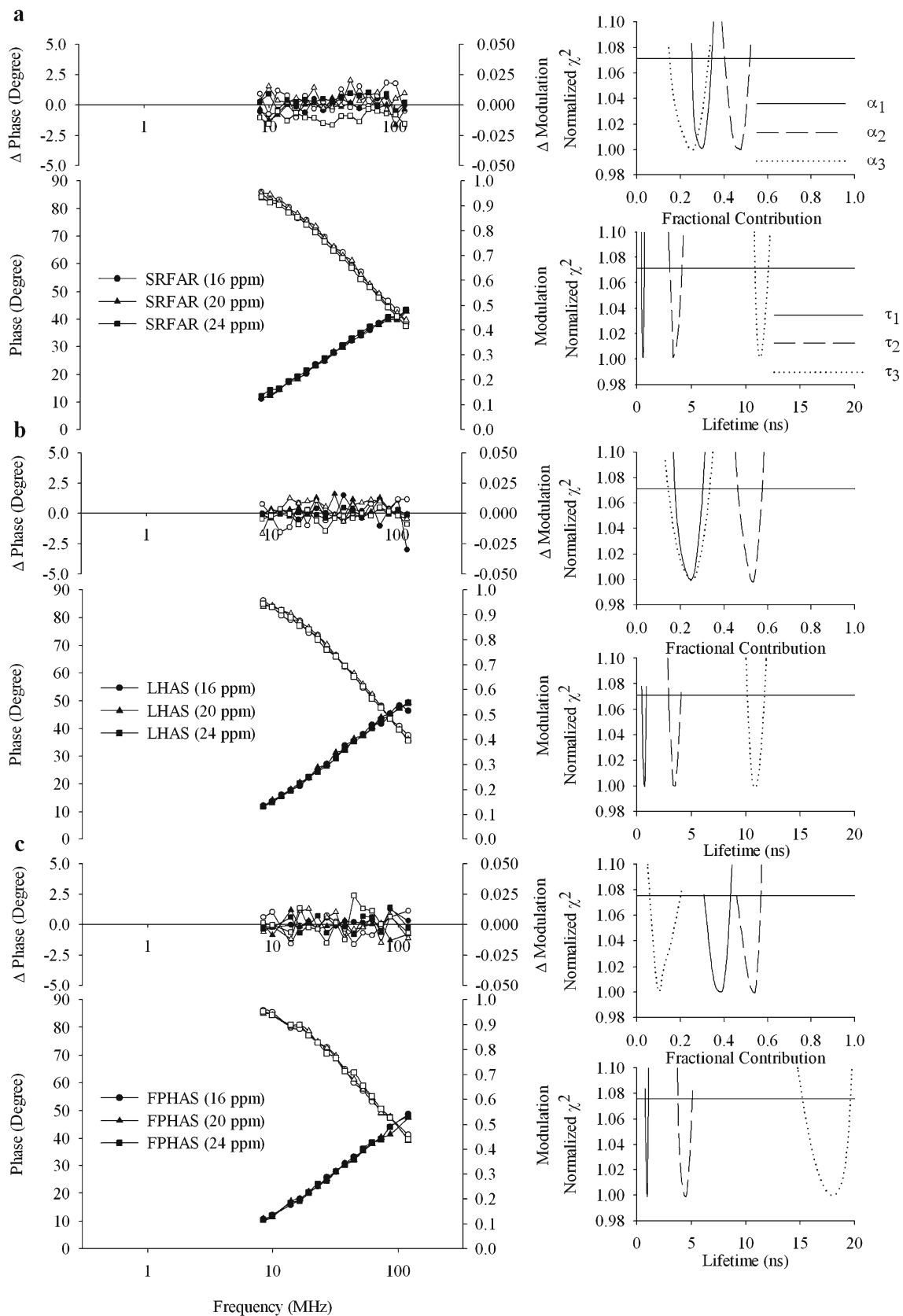


Fig. 1 Frequency-domain data and normalized χ^2 surfaces of NLLS analyses for **a** SRFAR, **b** LHAS, and **c** FPHAS. Solid and open symbols, in frequency-domain data, represent phase and modulation,

respectively. Horizontal solid lines: 1 SD from the minima of the χ^2 surface. Corresponding fitting parameters are tabulated in Table 1

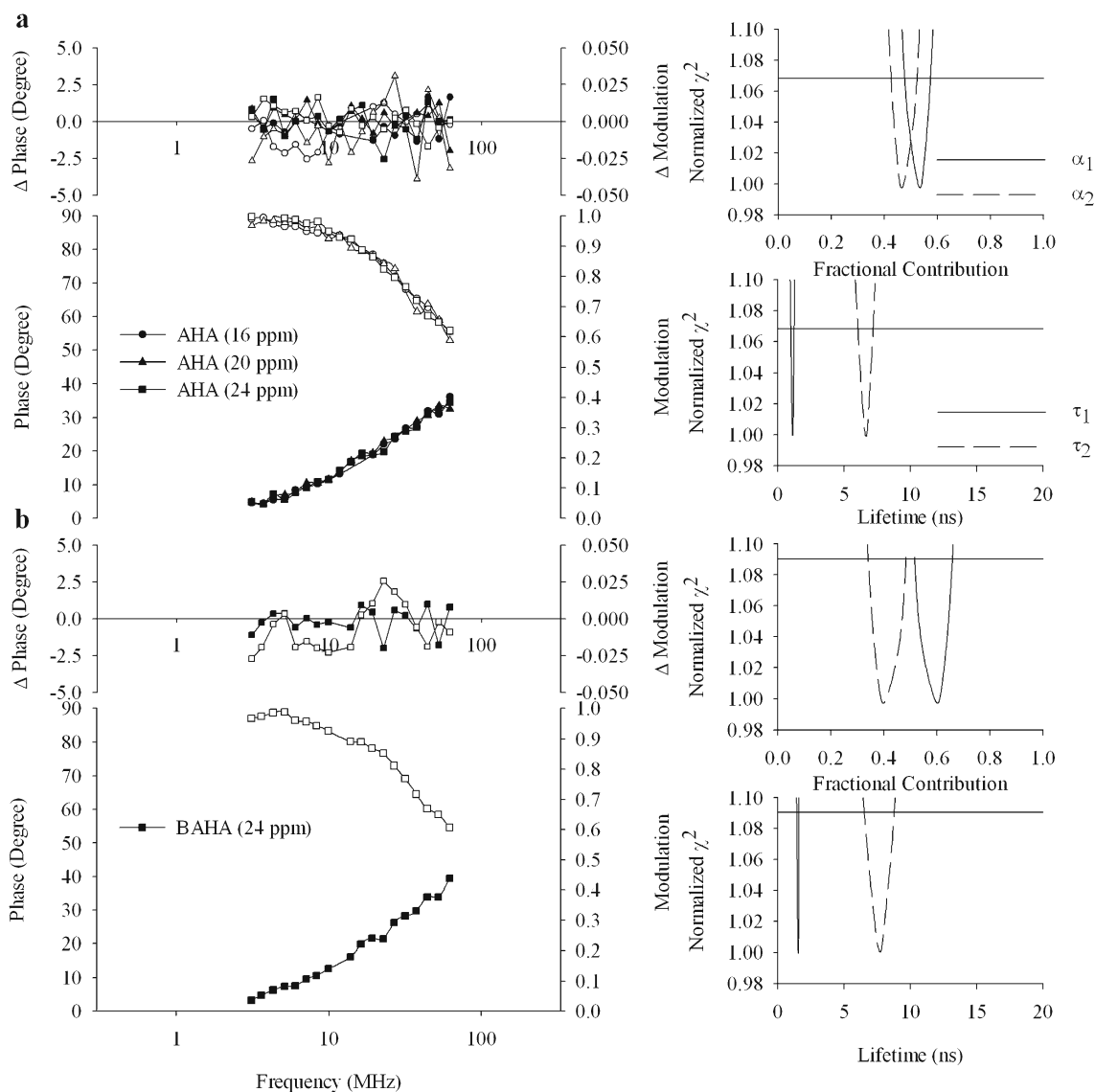


Fig. 2 Frequency-domain data and normalized χ^2 surfaces of NLLS analyses for **a** AHA and **b** BAHA. Solid and open symbols, in frequency-domain data, represent phase and modulation, respectively.

Horizontal solid lines: 1 SD from the minima of the χ^2 surface. Corresponding fitting parameters are tabulated in Table 1

and FPHAS) DHM (Fig. 1, Table 1 —Rows 2–4). However, a two-exponential decay (DD) model was found to be more stable and robust, as well as to provide the best fitting parameters for AHA (Fig. 2a, Table 1—Row 5). (See Supplementary information (SI) for a side-by-side comparison of Fig. 1a–c and Fig. 2a fits and residuals including 12 ppm data, Fig. 1S). The DD model was also found to be the most appropriate when fitting the data for 24 ppm BAHA (Fig. 2b, Table 1 —Row 6). The instability of the DDD model for both AHA and BAHA is further confirmed by the breadth of the χ^2 surfaces from the NLLS analyses for the DDD model (See SI, Fig. 2S). Addition of the third component did not significantly improve the χ^2 values. It should be noted that due to nature of HM, great care must be taken when interpreting the parameters from these fits,

as they are only operationally defined [42]. In the case of many DHM, a three component model has been required to adequately fit the experimental data. However, in the case of AHA and BAHA, two components appear to be sufficient.

The effect of concentration The suitability of DDD and DD models for argon degassed aqueous solution of the commercial and Amherst DHM, respectively, are also supported by the χ^2 surfaces of NLLS analyses (See SI, Fig. 3S) at various concentrations. From the χ^2 surfaces, it can be seen that both models are stable (relatively narrow surfaces converging to distinct minima) at all concentrations of each humic acid. Similar fractional contributions were obtained for all humic acid concentrations, except for 12 ppm, suggesting that both

Table 1 Recovered fluorescence lifetimes and fractional contributions obtained from NLLS analyses of pyrene, DHM, and their mixture

Model	[DHM] (ppm)	Set	α_{DHM}	α_1	τ_1 (ns)	α_2	τ_2 (ns)	α_3	τ_3 (ns)	α_4	τ_4 (ns)	χ^2
D	0	Pyrene	–	1.00	193.74	–	–	–	–	–	–	0.72
D _L D _L D _L	16–20–24	SRFAR	–	0.30	0.58	0.46	3.36	0.24	10.98	–	–	2.76
D _L D _L D _L	16–20–24	LHAS	–	0.24	0.70	0.52	3.32	0.24	10.59	–	–	2.25
D _L D _L D _L	16–20–24	FPHAS	–	0.38	0.95	0.53	4.36	0.09	16.61	–	–	2.52
D _L D _L	16–20–24	AHA	–	0.53	1.09	0.47	6.54	–	–	–	–	5.78
DD	24	BAHA	–	0.59	1.51	0.41	7.51	–	–	–	–	6.38
(D + D + D) _F D	16	PyreneSRFAR	0.41	0.30	0.58	0.46	3.36	0.24	10.98	0.59	185.95	2.27
(D + D + D) _F D	20	–	0.46	0.30	0.58	0.46	3.36	0.24	10.98	0.54	192.73	2.93
(D + D + D) _F D	24	–	0.73	0.30	0.58	0.46	3.36	0.24	10.98	0.27	178.38	3.33
(D + D + D) _F D	16	PyreneLHAS	0.75	0.24	0.70	0.52	3.32	0.24	10.59	0.25	204.59	3.63
(D + D + D) _F D	20	–	0.74	0.24	0.70	0.52	3.32	0.24	10.59	0.26	189.14	2.34
(D + D + D) _F D	24	–	0.80	0.24	0.70	0.52	3.32	0.24	10.59	0.20	190.97	3.71
(D + D + D) _F D	16	PyreneFPHAS	0.65	0.38	0.95	0.53	4.36	0.09	16.61	0.35	223.03	5.46
(D + D + D) _F D	20	–	0.71	0.38	0.95	0.53	4.36	0.09	16.61	0.29	226.63	4.22
(D + D + D) _F D	24	–	0.77	0.38	0.95	0.53	4.36	0.09	16.61	0.23	207.11	4.08
(D + D + D) _F D	16	PyreneAHA	0.36	0.53	1.09	0.47	6.54	–	–	0.64	190.11	7.40
(D + D + D) _F D	20	–	0.43	0.53	1.09	0.47	6.54	–	–	0.57	190.47	4.62
(D + D + D) _F D	24	–	0.54	0.53	1.09	0.47	6.54	–	–	0.46	193.80	3.80
(D + D + D) _F D	16	PyreneBAHA	0.14	0.59	1.51	0.41	7.51	–	–	0.86	192.88	7.17
(D + D + D) _F D	20	–	0.17	0.59	1.51	0.41	7.51	–	–	0.83	192.41	7.65
(D + D + D) _F D	24	–	0.20	0.59	1.51	0.41	7.51	–	–	0.80	194.94	5.93

The L subscripts correspond to the fits where both DHM fractional intensity contributions and lifetimes were linked during NLLS analyses. The F subscripts denote the fits where both the DHM fractional intensity contributions and lifetimes were fixed during NLLS analyses. Bolded black parameters are fixed values.

the nature and concentration of DHM influence their behavior and possibly their ultimate association with HOC. Rows 2–5 in Table 1 as well as χ^2 surfaces in Figs. 1 and 2 are global fits to data collected at 16, 20, and 24 ppm. Because a relatively stable state appears to be established for the concentration range between 16 to 24 ppm, data collected at 12 ppm were not included in the global analyses. In this examination, both the fractional contributions and lifetimes were allowed to vary but all parameters were linked for all three remaining concentrations of DHM individual components.

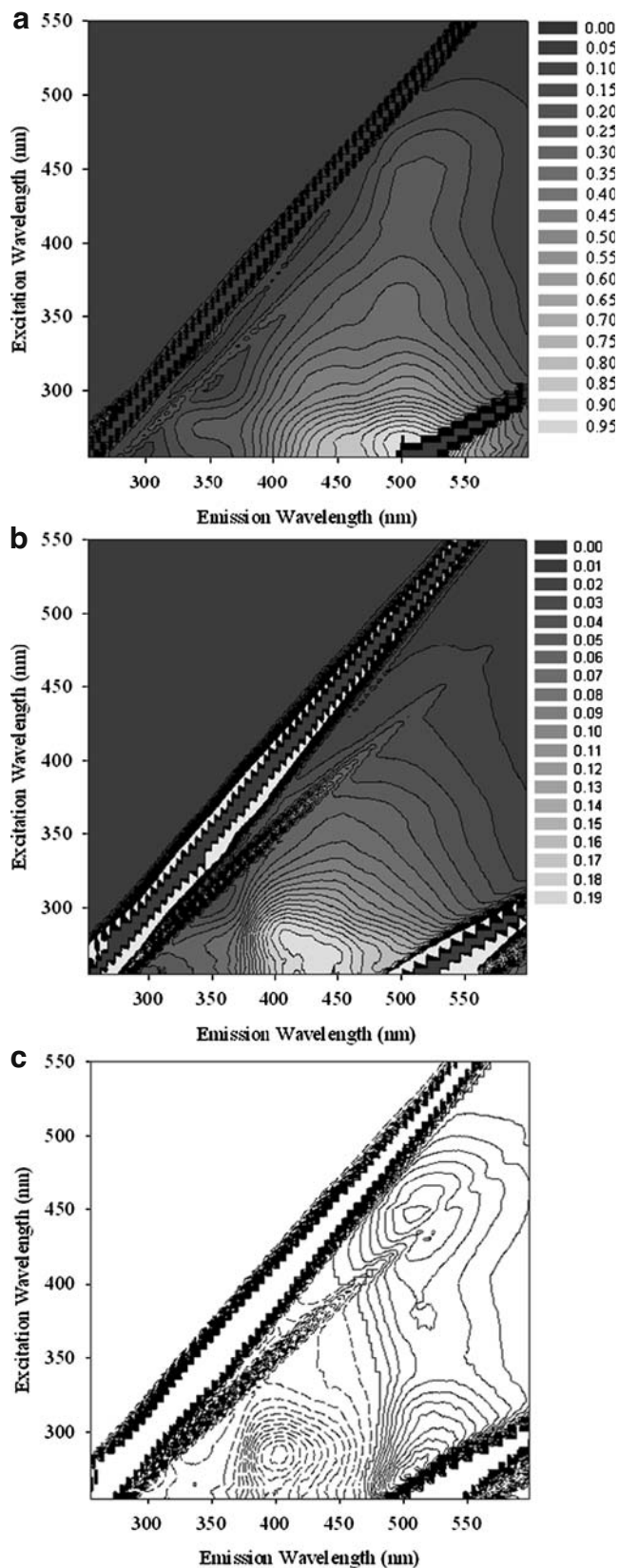
These findings are consistent with (1) previous reports that dissolved humic material assemblies are expanded and stretched sheet-like structures at low concentrations, and are folded and twisted at high concentrations [43, 44], and (2) the idea that exciplexes explain a large amount of the fluorescence exhibited by humic materials [45].

The effect of oxygen In this study, frequency-domain lifetime measurements were also obtained for air-equilibrated as well as argon de-gassed 24 ppm LHAS, used as a model of DHM, to evaluate the effect of oxygen on the recovered fractional contributions and lifetimes of DHM (See SI, Fig. 4S). The χ^2 surfaces of the NLLS analyses were also performed by allowing all parameters to vary. Only a small variation in the first and third lifetime components can be noted between the two samples. However, the highest probability of both

fractional intensity contributions and lifetimes are very similar for both the air-saturated and argon degassed LHAS solutions, as seen from the minima of the χ^2 surfaces. These findings are consistent with the fluorophores within the DHM being protected from the quenching effects of oxygen, and hence, proposed to be in the interior of the DHM assemblies.

The effect of chemical bleaching AHA was chemically bleached (to create BAHA) in an attempt to remove a large fraction of the aromatic entities [36]. The EEM spectra for the two samples are shown in Fig. 3. Analysis revealed that, per unit concentration, the BAHA was 80% less fluorescent as compared to the AHA sample. This was expected as a large fraction of the fluorescent aromatic moieties have been removed when AHA was bleached to yield BAHA [36]. Close inspection reveals that the chemical bleaching process preferentially removes longer wavelength emitting fluorophores. It has recently been proposed that the majority of the fluorescence is due to exciplexes of quinone moieties [45–47]. If this is that case then the results in Fig. 3c indicate that

Fig. 3 EEM spectra of **a** AHA normalized at its fluorescence maximum and **b** BAHA normalized at the maximum fluorescence of AHA EEM spectra. **c** The difference of AHA and BAHA EEM spectra estimated by subtracting the BAHA from AHA normalized EEM spectra at their individual emission maximum. *Solid and dash lines* represent positive and negative differences, respectively



the bleaching process removes either the more conjugated quinone moieties or quinone moieties in a less polar environment. The EEM spectra support the notion of the bleached quinone moieties being more conjugated, as a red shift is observed for both the $n-\pi^*$ and the $\pi-\pi^*$ excitation transitions, while arguing against these moieties being in different polar environments [48]. Also consistent with this view is the fact that the red shifted quinone moieties were bleached, and hence, were in a polar environment.

The data in Table 1 also hint that the bleaching process removes less of the ~ 1 ns lifetime fluorophore population. The combined EEM and lifetime results suggest that the less conjugated quinone population has shorter lifetimes than the more conjugated quinone population within AHA. Due to the unique fluorescence characteristics of the AHA sample (i.e.: two versus three lifetime components), it

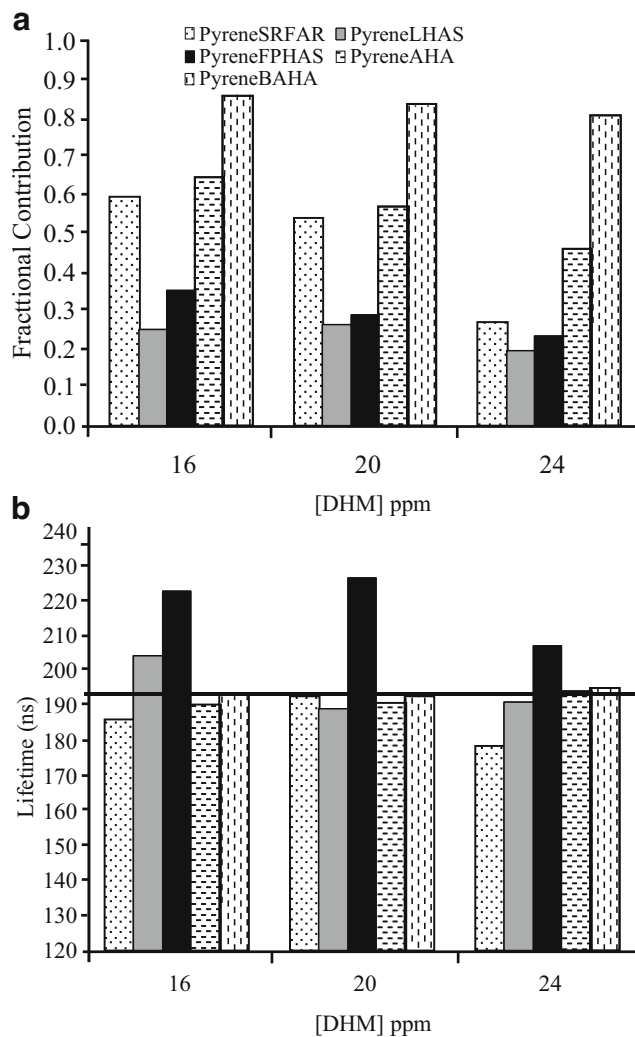


Fig. 4 Recovered pyrene **a** fractional contributions and **b** fluorescence lifetimes obtained from NLLS analyses for the $(D + D + D)_F D$ model of pyrene and DHM mixture. The *black solid line* indicates the measured pyrene lifetime in the absence of DHM. Corresponding fitting parameters are tabulated in Table 1

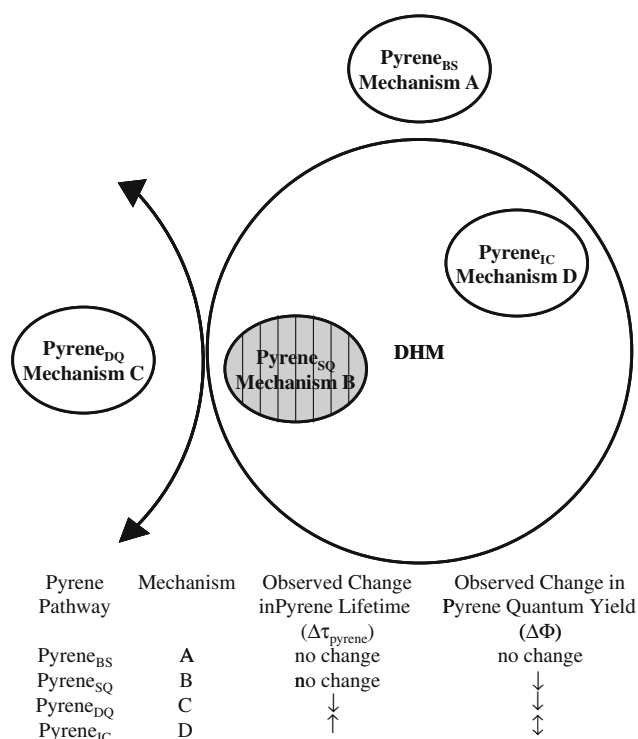


Fig. 5 Proposed model illustrating possible quenching mechanisms of pyrene in the presence of DHM. The subscript *BS* indicates the bulk solvent, *SQ* refers to static quenching, *DQ* is dynamic quenching, and *IC* denotes inclusion couple. The symbol ↓ indicates decrease, ↑ denotes an increase, and ↕ is decrease or increase

seems unwise to extrapolate this finding to natural organic matter as a whole, although it is interesting to note that a similar trend of short lifetimes being associated with shorter emission wavelengths has been previously reported for humic materials [39, 40].

Lifetime measurements of pyrene and DHM mixture

A range of measures were undertaken to greatly reduce or eliminate the effects of oxygen, HOC adsorption to cell walls, and concentration. The elimination of these factors greatly simplifies fluorescence measurements on systems as complex as DHM and their mixtures with HOC. Photobleaching within complex multi-component mixtures may also severely complicate data analysis and interpretation. This concern has traditionally not been addressed. Its omission may be valid for a single component (pyrene only) or if all components photobleach at the same rate. However, for systems such as pyrene with DHM, it was found that photobleaching needs to be accounted for and eliminated. This can be accomplished through specialized multi-harmonic-frequency (MHF) instrumentation such as the SLM-Amico 48,000 MHF which is no longer commercially available, or to a certain level via recent hardware improvements. For example, a variation of MHF instrumentation, the HORIBA Jobin Yvon MF², is capable

reducing sample exposure by collecting data at a high rate. However, a more practical solution for many laboratories uses more common, conventional, phase-modulation instrumentation while taking advantage of the frequency segmentation and recombination method previously described by Marwani et al. [32]. This is the method employed in this report.

Models for fitting data Pyrene and the commercial DHM mixtures are expected to show a minimum of four lifetimes (three for DHM and one pyrene). The $(D + D + D)_F D$ model was found here and previously [32] to be the most stable and robust model for the pyrene and the commercial DHM mixtures. In this model, both DHM fractions and lifetimes are fixed (F) at values determined from analysis of the individual DHM within the sum of three-exponential decays $(D + D + D)_F$, and pyrene fraction and lifetime is allowed to vary as a discrete (D) component model. A detailed discussion of the $(D + D + D)_F D$ model has been given by Marwani et al. [32]. The same logic was used as the basis for a $(D + D)_F D$ model for the pyrene and AHA or BAHA mixtures, as it was found that AHA and BAHA were best modeled by two components fits, as discussed above. These two models were then applied to analyze the segmented and re-combined (i.e. combined run) data from the pyrene/DHM mixtures for DHM ranging from 16–24 ppm. Recall that the confirmation of DHM may be concentration dependent (vide supra). Therefore, pyrene/DHM mixtures with DHM concentration of 12 ppm were not included in the analysis. Results are reported in Table 1—Rows 7–21.

Recovered pyrene fractional contribution Results of the recovered pyrene fractional contributions and lifetimes are provided graphically in Fig. 4. The χ^2 surfaces via NLLS analyses of pyrene and DHM mixtures were also evaluated in order to assess the range of statistically valid values for both the recovered pyrene fractional contributions and lifetimes (See SI, Fig. 5S). In general, for mixtures of pyrene with DHM, a decrease in the recovered fractional contributions of pyrene was observed with an increase in DHM concentration. This decrease was the most pronounced in the presence of LHAS, as compared to those with other DHM, which is indicative of the highest carbon and aromatic content of LHAS. The decrease in the recovered pyrene fractions was also found to be consistent with steady-state measurements (See SI, Figs. 6S and 7S), further supporting the model used to fit fluorescence lifetime data. It is of interest to note that the AHA recovered fractional contributions of pyrene were affected to a greater extent than those for BAHA, which is consistent with the higher aromatic content of AHA versus BAHA and suggests that there are specific aromatic moieties within the HM that quench pyrene fluorescence [10].

Fluorescence lifetime components The lifetime components of the fluorescence measurements allow for insight into the quenching mechanism from a different point of view than the steady-state data. The lifetime data for the systems under study in this report (pyrene, DHM and DHM/pyrene mixtures) are presented in Table 1, with the data related to pyrene mixtures over the DHM concentration range of 16–24 ppm for all five HM studied (Table 1—Rows 7–21) presented graphically in Fig. 4. See SI, Fig. 5S for χ^2 surfaces. From these data it can be seen that the DHM concentration appears to influence the lifetime of pyrene. The lifetimes of pyrene in the presence of 16 to 20 ppm SRFAR are very close to those of neat pyrene (~194 ns). However, for 24 ppm, an appreciably shorter lifetime is found. These data are consistent with *static* quenching dominating at the two lower concentrations, and *dynamic* quenching becoming an appreciable quenching mechanism at a concentration of 24 ppm SRFAR. For both AHA and BAHA, the pyrene lifetime is found to be very close to that of pyrene in the absence of DHM, which is consistent with static quenching being the dominant quenching mechanism at work in the studied concentration range of AHA and BAHA. A very different picture emerges when the lifetime data for pyrene in the presence of FPHAS are considered. These data show that the lifetime of pyrene has increased to 223, 227, and 207 ns in the presence of 16, 20, and 24 ppm FPHAS, respectively. These lifetimes are appreciably greater than those found for pyrene in the absence of DHM. This enhancement of pyrene's lifetimes is not consistent with either static or dynamic quenching. Recall that the fractional contributions and supporting information (SI Fig. 6S) discussed above show a decrease in pyrene fluorescence with increasing FPHAS concentration. This increase in measured pyrene lifetime combined with a decrease pyrene emission means that a new mechanism appears to be at work, and is indicative of pyrene movement toward different microenvironments within DHM. The 16 ppm data for SRFAR also hint at an enhancement of pyrene's lifetime. An inclusion 'couple' between the pyrene and FPHAS may explain the longer lifetimes, akin to the inclusion complex found for the association of pyrene with γ -cyclodextrin [49]. Nelson et al. [49] argued that due to the complexation γ -cyclodextrin protected pyrene from a number of fluorescence deactivation pathways, shielded pyrene from the bulk aqueous environment, and increased the rigidity of pyrene.

Implications This finding means that the modeling of the fluorescence characteristics of pyrene, and quite possibly, also of a range of other polyaromatic compounds—when in association with DHM, must be amended, as illustrated in Fig. 5. Traditionally, pyrene fluorescence in the presence of DHM was modeled to reflect a complete quenching of the

fluorescence of the pyrene associated with the DHM, as illustrated in Fig. 5 by mechanisms A (no quenching; pyrene in bulk solvent) and B (traditional static quenching). More recently [15, 35], a fraction of the observed decrease in pyrene fluorescence has been assigned to dynamic quenching processes, mechanism C in Fig. 5. None of these mechanisms account for the decreased pyrene intensity combined with enhanced fluorescence lifetimes observed in this study. This has led to the incorporation of an additional mechanism in the proposed model. This mechanism involves an *inclusion* 'couple' between pyrene and DHM, mechanism D in Fig. 5. This inclusion 'couple' increases the measured lifetime of pyrene, while traditional static and dynamic quenching (mechanisms B and C) decrease the intensity of pyrene. It is therefore possible all mechanisms are at play, counteracting each other, thus making the measured pyrene lifetime no longer representative of any single mechanism or pyrene population. Stated in another way, there is a "tug of war" between mechanisms C and D in terms of pyrene measured lifetime, decreasing the probability of detecting either mechanism via lifetime measurements. These different quenching mechanisms are also consistent with a range of microenvironments within the DHM, which is consistent with the complex, heterogeneous, polydisperse and molecular assembly nature of humic materials.

Implications for the FQ method As stated above, the FQ method, used to determine the association constants for HOC with DHM, assumes a *dark*, statically quenched state for any pyrene associated with DHM. It has been argued that the same lifetimes obtained for pyrene in the presence and absence of DHM constitute a definitive proof of this assumption. The results presented here show how such lifetime data can be explained by a combination of mechanisms (e.g. mechanisms B–D in Fig. 5). This combination of mechanisms can also explain: (1) the positive curvature in Stern–Volmer plots (due to the previously unaccounted for dynamically quenched pyrene); (2) the fact that the binding constants afforded by the FQ method are consistently higher than those obtained by other methods (again, due to the previously unaccounted for dynamic quenching), and (3) the use of pyrene to monitor the polarity of DHM (e.g. the unaccounted for pyrene inclusion 'couple' is sensitive to its environment, thus changing its band structure) discussed in the Introduction above.

Conclusions

By studying a range of dissolved humic materials at different concentrations and their association with pyrene

by steady-state and time resolved fluorescence methods, the following was found:

- 1) The three IHSS humic samples were fitted by three lifetime components, consistent with previous findings. However, the AHA and BAHA samples were best fitted by a two lifetime component model.
- 2) The chemical bleaching of AHA to yield BAHA removed long wavelength emitting fluorophores, which appear to be more conjugated quinone moieties.
- 3) Each of the humic acids caused unique fluorescence quenching of pyrene, except for AHA and BAHA. Therefore proposed quenching mechanisms cannot be generalized to all DHM.
- 4) There is evidence of dissolved SRFAR dynamically quenching pyrene, as evidenced by the appreciable shorter lifetime (~178 ns) found in the presence of SRFAR compared to that found in the absence of DHM (~194 ns).
- 5) For pyrene associated with FPHAS, the measured lifetime was longer (>220 ns) than that for pyrene in the bulk solution, and was proposed to be due to the hydrophobic microenvironment provided by this humic material.

The FQ technique used to monitor polyaromatic hydrocarbon association with DHM, and its central assumption of a dark static quenching of pyrene when it associates with DHM, is inconsistent with the enhancement of pyrene lifetime seen here for FPHAS and the shorter pyrene lifetime found for pyrene with SRFAR. This leads to the suggestion that the FQ method be approached with great caution. In addition, the different fluorescence behavior for the different DHM studied here lead to the suggestion that, given the range of quenching mechanisms that are possible in the presence of DHM, the validity of the FQ method be confirmed for each DHM to be studied.

Acknowledgments Robert L. Cook acknowledges the Louisiana Education Quality Support Fund (LEQSF [2004–07]-RD-A-07), the National Science Foundation (CHE-0547982), and the United States Department of Agriculture (CSRESS 2005-35107-15278). Isiah M. Warner acknowledges the National Science Foundation, the National Institutes of Health, and the Philip W. West Endowment for their support.

References

1. Buffle J (1981) Complexation reactions in aquatic systems: an analytical approach, Ellis Horwood, Chichester, 1st edn. Ellis Horwood, Ltd., UK
2. Stevenson FJ (1994) Humus chemistry: genesis, composition, reactions, 2nd edn. Wiley, New York
3. Xing B, Pignatello JJ, Gigliotti B (1996) Competitive sorption between atrazine and other organic compounds in soils and model sorbents. *Environ Sci Technol* 30(8):2432–2440
4. Weber WJ Jr, Huang W (1996) A distributed reactivity model for sorption by soils and sediments. 4. Intraparticle heterogeneity and phase-distribution relationships under nonequilibrium conditions. *Environ Sci Technol* 30(3):881–888
5. Huang W, Weber WJ Jr (1997) A distributed reactivity model for sorption by soils and sediments. 10. Relationships between desorption, hysteresis, and the chemical characteristics of organic domains. *Environ Sci Technol* 31(9):2562–2569
6. Xing B, Pignatello JJ (1997) Dual-mode sorption of low-polarity compounds in glassy poly(vinyl chloride) and soil organic matter. *Environ Sci Technol* 31(3):792–799
7. Huang W, Young TM, Schlautman MA, Yu H, Weber WJ Jr (1997) A distributed reactivity model for sorption by soils and sediments. 9. General isotherm nonlinearity and applicability of the dual reactive domain model. *Environ Sci Technol* 31(6):1703–1710
8. Graber ER, Borisover MD (1998) Evaluation of the glassy/rubbery model for soil organic matter. *Environ Sci Technol* 32(21):3286–3292
9. Engebretson RR, von Wandruszka R (1994) Micro-organization in dissolved humic acids. *Environ Sci Technol* 28(11):1934–1941
10. Chin Y-P, Aiken GR, Danielsen KM (1997) Binding of pyrene to aquatic and commercial humic substances: the role of molecular weight and aromaticity. *Environ Sci Technol* 31(6):1630–1635
11. Chiou CT, McGroddy SE, Kile DE (1998) Partition characteristics of polycyclic aromatic hydrocarbons on soils and sediments. *Environ Sci Technol* 32(2):264–269
12. Perminova IV, Grechishcheva NY, Petrosyan VS (1999) Relationships between structure and binding affinity of humic substances for polycyclic aromatic hydrocarbons: relevance of molecular descriptors. *Environ Sci Technol* 33(21):3781–3787
13. Perminova IV, Grechishcheva NY, Kovalevskii DV, Kudryavtsev AV, Petrosyan VS, Matorin DN (2001) Quantification and prediction of the detoxifying properties of humic substances related to their chemical binding to polycyclic aromatic hydrocarbons. *Environ Sci Technol* 35(19):3841–3848
14. Drewes JE, Croue JP (2002) New approaches for structural characterization of organic matter in drinking water and wastewater effluents. *Water Sci Technol: Water Supply* 2(2):1–10
15. Holbrook RD, Love NG, Novak JT (2004) Investigation of sorption behavior between pyrene and colloidal organic carbon from activated sludge processes. *Environ Sci Technol* 38(19):4987–4994
16. Chefetz B, Deshmukh AP, Hatcher PG, Guthrie EA (2000) Pyrene sorption by natural organic matter. *Environ Sci Technol* 34(14):2925–2930
17. Hu W-G, Mao J, Xing B, Schmidt-Rohr K (2000) Poly(methylene) crystallites in humic substances detected by nuclear magnetic resonance. *Environ Sci Technol* 34(3):530–534
18. Wang K, Xing B (2005) Structural and sorption characteristics of adsorbed humic acid on clay minerals. *J Environ Qual* 34(1):342–349
19. Sutton R, Sposito G (2005) Molecular structure in soil humic substances: the new view. *Environ Sci Technol* 39(23):9009–9015
20. Lakowicz JR (1999) Principles of fluorescence spectroscopy, 2nd edn. Kluwer Academic/Plenum, New York
21. Gauthier TD, Shane EC, Guerin WF, Seitz WR, Grant CL (1986) Fluorescence quenching method for determining equilibrium constants for polycyclic aromatic hydrocarbons binding to dissolved humic materials. *Environ Sci Technol* 20(11):1162–1166
22. Puchalski MM, Morra MJ, Von Wandruszka R (1992) Fluorescence quenching of synthetic organic compounds by humic materials. *Environ Sci Technol* 26(9):1787–1792
23. Doll TE, Frimmel FH, Kumke MU, Ohlenbusch G (1999) Interaction between natural organic matter (NOM) and polycyclic

- aromatic compounds (PAC). Comparison of fluorescence quenching and solid phase micro extraction (SPME). *Fresenius J Anal Chem* 364(4):313–319
24. Laor Y, Rebhun M (2002) Evidence for nonlinear binding of PAHs [polycyclic aromatic hydrocarbons] to dissolved humic acids. *Environ Sci Technol* 36(5):955–961
 25. Peuravuori J (2001) Partition coefficients of pyrene to lake aquatic humic matter determined by fluorescence quenching and solubility enhancement. *Anal Chim Acta* 429(1):65–73
 26. Pan B, Xing B, Liu W, Xing G, Tao S (2007) Investigating interactions of phenanthrene with dissolved organic matter: limitations of Stern–Volmer plot. *Chemosphere* 69(10):1555–1562
 27. Mackenzie K, Georgi A, Kumke M, Kopinke F-D (2002) Sorption of pyrene to dissolved humic substances and related model polymers. 2. Solid-phase microextraction (SPME) and fluorescence quenching technique (FQT) as analytical methods. *Environ Sci Technol* 36(20):4403–4409
 28. Ganaye VA, Keiding K, Viriot M-L, Vogel TM, Block J-C (1997) Evaluation of soil organic matter polarity by pyrene fluorescence spectrum variations. *Environ Sci Technol* 31(10):2701–2706
 29. Sierra MMD, Rauen TG, Tormen L, Debacher NA, Soriano-Sierra EJ (2005) Evidence from surface tension and fluorescence data of a pyrene-assisted micelle-like assemblage of humic substances. *Water Res* 39(16):3811–3818
 30. Backhus DA, Golini C, Castellanos E (2003) Evaluation of fluorescence quenching for assessing the importance of interactions between nonpolar organic pollutants and dissolved organic matter. *Environ Sci Technol* 37(20):4717–4723
 31. Tiller CL, Jones KD (1997) Effects of dissolved oxygen and light exposure on determination of K_{oc} values for PAHs using fluorescence quenching. *Environ Sci Technol* 31(2):424–429
 32. Marwani HM, Lowry M, Keating P, Warner IM, Cook RL (2007) Segmented frequency-domain fluorescence lifetime measurements: minimizing the effects of photobleaching within a multi-component system. *J Fluoresc* 17(6):687–699
 33. Chen S, Inskeep WP, Williams SA, Callis PR (1994) Fluorescence lifetime measurements of fluoranthene, 1-naphthol, and napropamide in the presence of dissolved humic acid. *Environ Sci Technol* 28(9):1582–1588
 34. Kumke MU, Loehmannsroeben HG, Roch T (1995) Fluorescence spectroscopy of polynuclear aromatic compounds in environmental monitoring. *J Fluoresc* 5(2):139–153
 35. Nakashima K, Maki M, Ishikawa F, Yoshikawa T, Gong YK, Miyajima T (2007) Fluorescence studies on binding of pyrene and its derivatives to humic acid. *Spectrochim Acta, Part A: Mol Biomol Spectrosc* 67A(3–4):930–935
 36. Gunasekara AS, Simpson MJ, Xing B (2003) Identification and characterization of sorption domains in soil organic matter using structurally modified humic acids. *Environ Sci Technol* 37(5):852–858
 37. Beechem JM (1989) A second generation global analysis program for the recovery of complex inhomogeneous fluorescence decay kinetics. *Chem Phys Lipids* 50(3–4):237–251
 38. Beechem JM, Gratton E (1988) Fluorescence spectroscopy data analysis environment: a second generation global analysis program. *Proceedings of SPIE-The International Society for Optical Engineering* 909 (Time-Resolved Laser Spectrosc. Biochem.):70–81
 39. Cook RL, Langford CH (1995) Metal ion quenching of fulvic acid fluorescence intensities and lifetimes: Nonlinearities and a possible three-component model. *Anal Chem* 67(1):174–180
 40. Hemmingsen SL, McGown LB (1997) Phase-resolved fluorescence spectral and lifetime characterization of commercial humic substances. *Appl Spectrosc* 51(7):921–929
 41. Hewitt JD, McGown LB (2003) On-the-fly fluorescence lifetime detection of humic substances in capillary electrophoresis. *Appl Spectrosc* 57(3):256–265
 42. Kumke MU, Tiseanu C, Abbt-Braun G, Frimmel FH (1998) Fluorescence decay of natural organic matter (NOM)—influence of fractionation, oxidation, and metal ion complexation. *J Fluoresc* 8(4):309–318
 43. Piccolo A, Conte P, Trivellone E, van Lagen B, Buurman P (2002) Reduced heterogeneity of a lignite humic acid by preparative hpsc following interaction with an organic acid. Characterization of size-separates by PYR-GC-MS and ^1H NMR spectroscopy. *Environ Sci Technol* 36(1):76–84
 44. Lee C-L, Kuo L-J, Wang H-L, Hsieh P-C (2003) Effects of ionic strength on the binding of phenanthrene and pyrene to humic substances: three-stage variation model. *Water Res* 37(17):4250–4258
 45. Ariese F, Van Assema S, Gooijer C, Bruccoleri AG, Langford CH (2004) Comparison of Laurentian fulvic acid luminescence with that of the hydroquinone/quinone model system: evidence from low temperature fluorescence studies and EPR spectroscopy. *Aquatic Sciences* 66(1):86–94
 46. Del Vecchio R, Blough NV (2004) On the origin of the optical properties of humic substances. *Environ Sci Technol* 38(14):3885–3891
 47. Cory RM, McKnight DM (2005) Fluorescence spectroscopy reveals ubiquitous presence of oxidized and reduced quinones in dissolved organic matter. *Environ Sci Technol* 39(21):8142–8149
 48. Turro NJ (1991) *Modern molecular photochemistry*, 1st edn. University Science Books, California
 49. Nelson G, Patonay G, Warner IM (1988) Effects of selected alcohols on cyclodextrin inclusion complexes of pyrene using fluorescence lifetime measurements. *Anal Chem* 60(3):274–279